

# Redesigning the mechanism of the lipase-catalysed aminolysis of esters

Javier González-Sabín, Iván Lavandera, Francisca Rebolledo\* and Vicente Gotor\*

*Departamento de Química Orgánica e Inorgánica, Universidad de Oviedo, 33071 Oviedo, Spain*

Received 15 March 2006; accepted 15 April 2006

**Abstract**—In a previous work, several 2-phenylcycloalkanamines were subjected to aminolysis catalysed by the lipase B from *Candida antarctica* (CAL-B). In these processes, the size of the cycle and the stereochemistry of the stereogenic centres of the amines had a strong influence on both the enantiomeric ratio and the reaction rate. Herein, molecular modelling approaches have been used to revise the lipase-catalysed aminolysis mechanism. Thus, complexes of CAL-B with the phosphoramidate analogues related to substrates in the kinetic resolution of several 2-phenylcycloalkanamines by this enzyme were built and minimised. This computational study suggests the formation of zwitterionic species (named TI-Z), resulting from the direct His-unassisted attack of the amine onto the carbonyl group of the acyl-enzyme, as the most plausible intermediate for the CAL-B-catalysed aminolysis. This proposal differs slightly from the commonly accepted serine-mediated mechanism, where removal of the proton from the amine occurs simultaneously to the nucleophile attack to the acyl-enzyme complex (TI-2). Subsequently, His-assisted deprotonation of the resulting ammonium group takes place, and a molecule of water could be necessary in some cases to facilitate the transfer of the proton to the catalytic histidine.  
© 2006 Elsevier Ltd. All rights reserved.

## 1. Introduction

The aminolysis of esters is a model reaction between an electrophile and a nucleophile that has been subjected to a great number of experimental and theoretical studies.<sup>1</sup> Base-catalysed models of this reaction have previously been reported by Bruice and Mayahi,<sup>2</sup> Jencks and Carriulo,<sup>3</sup> and Bunnett and Davis.<sup>4</sup> The mechanism has been widely revised and, even today, there is not a definitive outcome. Thus, in general, three different pathways have been considered when this reaction has been studied: (a) the concerted mechanism, where the transfer of the proton from the amine to the leaving group occurs simultaneously to the cleavage and formation of the bonds involved in the process; (b) the stepwise mechanism where no charged-intermediates are present (the typical ‘addition/elimination’ pathway) and (c) the stepwise mechanism through zwitterionic species.

The lipase-catalysed acylation of amines is an example of an aminolysis process assisted by a weak base.<sup>5</sup> Although this reaction has been widely used to obtain optically active amines,<sup>6</sup> in some cases on a multi-ton scale,<sup>7</sup> its mechanism

has scarcely been studied, and it is assumed, and therefore accepted that the pathway for acylation of amines is completely analogous to that for acylation of alcohols (serine-mediated mechanism).<sup>8</sup> In spite of the higher nucleophilicity of amines compared to alcohols, most hydrolase-catalysed acylations involve alcohols not amines. Further, reactions with amines are often slower, requiring larger amounts of catalyst or longer reaction times.

In the last few years, we have investigated the utility of some lipases, especially the lipase B from *Candida antarctica* (CAL-B) to catalyse the enantio-,<sup>9</sup> and regioselective<sup>10</sup> aminolysis of esters. Thus, we have recently described the CAL-B-catalysed kinetic resolutions of racemic *trans*- and *cis*-2-phenylcycloalkanamines *rac*-1–*rac*-5 (Fig. 1).<sup>11</sup> These types of substrates are very interesting due to their pharmacological properties<sup>12</sup> and also due to their potential applicability as chiral auxiliaries, bases and ligands.

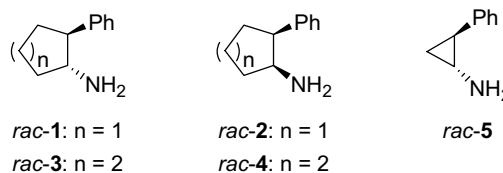


**Figure 1.** 2-Phenylcycloalkanamines.

\* Corresponding authors. Tel./fax: +34 98 510 3448; e-mail addresses: [FRV@fq.uniovi.es](mailto:FRV@fq.uniovi.es); [VGS@fq.uniovi.es](mailto:VGS@fq.uniovi.es)

The efficacy of the CAL-B-catalysed resolution of 2-phenylcycloalkanamines was dramatically influenced by the stereochemistry and the size of the cycle of the amine (Table 1).<sup>11</sup> When the resolution of *rac-1–rac-5* was carried out by CAL-B-catalysed acylation under the simplest reaction conditions, that is using ethyl acetate as the acyl donor and the solvent, (1*R*,2*S*)-enantiomers of *trans* derivatives *rac-1* and *rac-3* (Table 1, entries 1 and 3) were acetylated following the Kazlauskas' rule,<sup>13</sup> however poor results were obtained for their *cis* counterparts *rac-2*, and especially for *rac-4*, for which the acylation was markedly slower and not enantioselective (Table 1, entries 2 and 4).<sup>14</sup> Finally, the enantioselectivity of the process with the amine *rac-5* (Table 1, entry 5) was very low ( $E = 3.5$ ) and proceeded smoothly, accomplishing a very high conversion degree ( $c = 90\%$ ) after only 2 h of reaction. We took these processes as models to gain insight into the aminolysis reaction.

**Table 1.** CAL-B-catalysed resolution of racemic 2-phenylcycloalkanamines<sup>a,b</sup>

Entry	Amine	Time (h)	$c$ (%)	Configuration of the fast-reacting enantiomer	$E$
1	<i>rac-1</i>	6.5	50	(1 <i>R</i> ,2 <i>S</i> )	>200
2	<i>rac-2</i>	24	28	(1 <i>R</i> ,2 <i>R</i> )	16
3	<i>rac-3</i>	20	41	(1 <i>R</i> ,2 <i>S</i> )	166
4	<i>rac-4</i>	47	5	—	≈1
5	<i>rac-5</i>	2	90	(1 <i>R</i> ,2 <i>S</i> )	4

<sup>a</sup> See Ref. 11.

<sup>b</sup> All reactions were carried out at 28 °C, 200 rpm, using ethyl acetate as the acyl donor and solvent.

Herein we have revisited the accepted serine-mediated mechanism for the hydrolase-catalysed acylation of amines, comparing it by means of a molecular modelling study with a related pathway where zwitterionic intermediates are involved. Our findings support this novel mechanism as the most plausible to explain the CAL-B-catalysed acylation of 2-phenylcycloalkanamines.

## 2. Results and discussion

Taking into account the scarcity of computer modelling studies about the aminolysis reaction,<sup>15</sup> we used this tool to rationalise the great differences in reactivity and enantio-

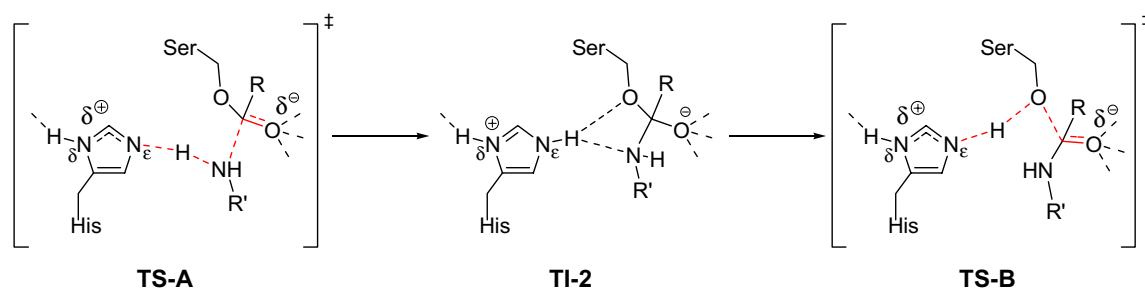
selectivity shown by CAL-B towards these cycloalkanamines. In recent years, molecular modelling has been successfully used to explain both the mechanism of action and the substrate selectivity of lipases.<sup>16</sup>

We started from an X-ray crystal structure of CAL-B<sup>17</sup> and used the AMBER force field, which is one of the most adequate for the study of proteins.<sup>18</sup> This lipase presents a typical serine-dependent catalytic triad, which is accessible from the solvent through a narrow channel. The X-ray structure of CAL-B was elucidated in 1994 by Uppenberg et al.,<sup>19</sup> and presents a small active site that restricts the possible orientations of the substrate: the acyl moiety of the substrate lies in the large hydrophobic pocket (or acyl pocket), while the nucleophile moiety is placed in the medium pocket (so called nucleophile or stereoselective), although it may extend into the solvent and/or into the large subsite.

Assuming that aminolysis and transesterification reactions proceed through a similar mechanism (Scheme 1), the enantiodiscrimination in this process has to be determined by one or both of the transition states involved in the formation (TS-A) or collapse (TS-B) of the second tetrahedral intermediate (TI-2). For this reason we modelled a phosphonamidate<sup>15</sup> (Fig. 2A) as an analogue of the tetrahedral intermediate TI-2 resulting from attack of the amine to the carbonyl of the acyl-enzyme. This intermediate is the equivalent to the phosphonate analogues successfully employed in the molecular modelling studies on the transesterification of alcohols.<sup>20</sup>

In the first stage, docking, charge parameterisation and geometry optimisation of the phosphonamidate analogue corresponding to the acetylation of ethylamine, formed all six essential hydrogen bonds for catalysis, and then, in a stepwise fashion, the cycle and the phenyl ring were added. Since the structure contained only two rotatable bonds, a careful systematic search identified the catalytically productive conformations, applying a methodical approach of releasing different motifs as described in the Experimental. We defined a catalytically productive conformation as one that presents all the key-catalytic hydrogen bonds (Fig. 2), a stable ring conformation, and avoids steric clashes between the phosphonamidate and the lipase.

For better understanding, this section has been divided into three subheadings. First, the molecular modelling study of



**Scheme 1.** Mechanism for the lipase-catalysed aminolysis based on the analogue for the transesterification reaction.

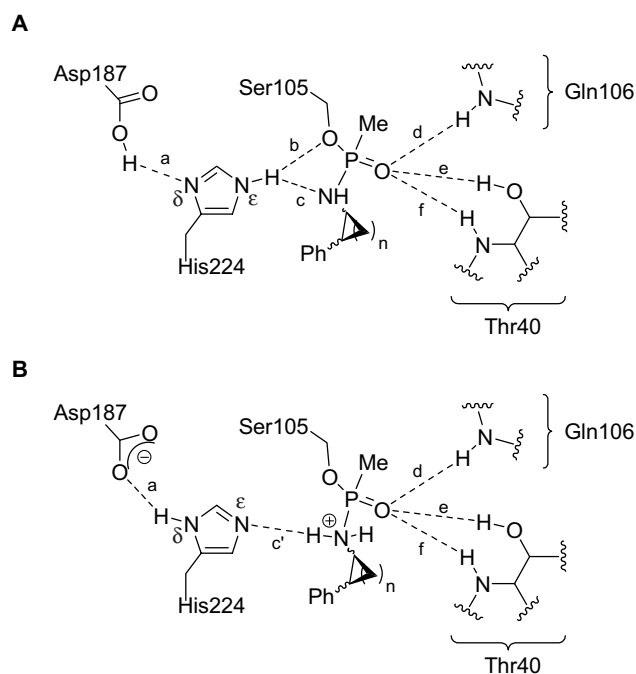


**Figure 2.** Analogues used in the molecular modelling study of the CAL-B-catalysed acetylation of 2-phenylcycloalkanamines mimicking: (A) TI-2 and (B) TI-Z. Essential hydrogen bonds for the catalysis are shown as dashed lines (a–f).

2-phenylcyclopentanamines *rac*-1 and *rac*-2, then of *trans*-2-phenylcyclopropanamine *rac*-5, and lastly, of 2-phenylcyclohexanamines *rac*-3 and *rac*-4 will be shown.

### 2.1. 2-Phenylcyclopentanamines *rac*-1 and *rac*-2

We started this study with the *trans*-diastereoisomer *rac*-1 (Fig. 1) that had been perfectly resolved by CAL-B,<sup>11a</sup> and tried to find a catalytically productive conformation for the fast-reacting enantiomer (1*R*,2*S*)-1 (Table 1, entry 1). Thus, the phosphoramidate analogue of TI-2 for (1*R*,2*S*)-1 was modelled. However, although several arrangements of the substrate in the active site were examined, non-productive conformations were found. The minimal distance found for the bond *c* between the N<sub>ε</sub>-H of His224 and the N of the nucleophile was still too large

(3.49 Å, Table 2, entry 1) for an H-bond interaction to exist.<sup>21</sup> This result indicates that the concerted attack of the amine on the acyl-enzyme carbonyl with the proton removal by the catalytic histidine is not favoured, and as a consequence, a different mechanism to that operating in the transesterification of alcohols might be plausible.

Looking at the literature, computational studies related to the aminolysis process have shown that stepwise mechanisms are usually more energetically favoured than the concerted one, and in some cases, it takes place through zwitterionic species. Thus, Adalsteinsson and Bruice,<sup>22</sup> investigated the intramolecularly catalysed aminolysis of substituted phenyl esters of quinoline derivatives. In these reactions assisted by a weak base, computational approaches demonstrated that the mechanism going via zwitterionic intermediates was the most favourable. They modelled the ammonolysis of compound **6**, which was used as a model of a quinoline carboxylic ester, obtained as the lowest energy pathway for the ammonia attack that is shown in Scheme 2.

In the case of the lipase-catalysed aminolysis, zwitterionic species<sup>23</sup> could be favoured if we consider the following facts: (1) the proton removal catalysed by a base, such as imidazole, from alcohols is much easier than from amines; (2) amines are stronger nucleophiles than alcohols and (3) the acyl-enzyme complex is a particularly activated ester due to the side chains of the amino acids that shape the oxyanion hole. Thus, we studied the direct attack of the amine to the acyl-enzyme carbonyl without the initial participation of the catalytic His (Scheme 3). The result was a tetrahedral intermediate that we have named as 'zwitterionic tetrahedral intermediate' (TI-Z),<sup>24</sup> which can go on to TI-2<sup>25</sup> by the subsequent His-mediated removal of the proton. In the last step, the transfer of the proton between [His-H]<sup>+</sup> and Ser takes place, to afford the amide.

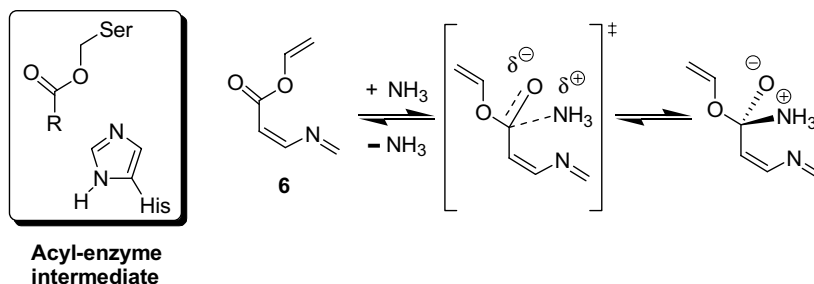
Assuming this pathway, enantiodiscrimination could be determined by TS-C, TS-D or both. Thus, we decided to model the protonated phosphoramidate analogue that would mimic TI-Z (Fig. 2B). This intermediate presents five key-hydrogen bonds, *c'* being essential for the subsequent His-mediated removal of the proton. In this case a catalytically productive conformation was defined as one that maintains all five key-hydrogen bonds presented in

**Table 2.** Distances and angles of the key hydrogen bonds in the most productive conformations obtained for the intermediates in the CAL-B-catalysed acetylation of *rac*-1, *rac*-2 and *rac*-5

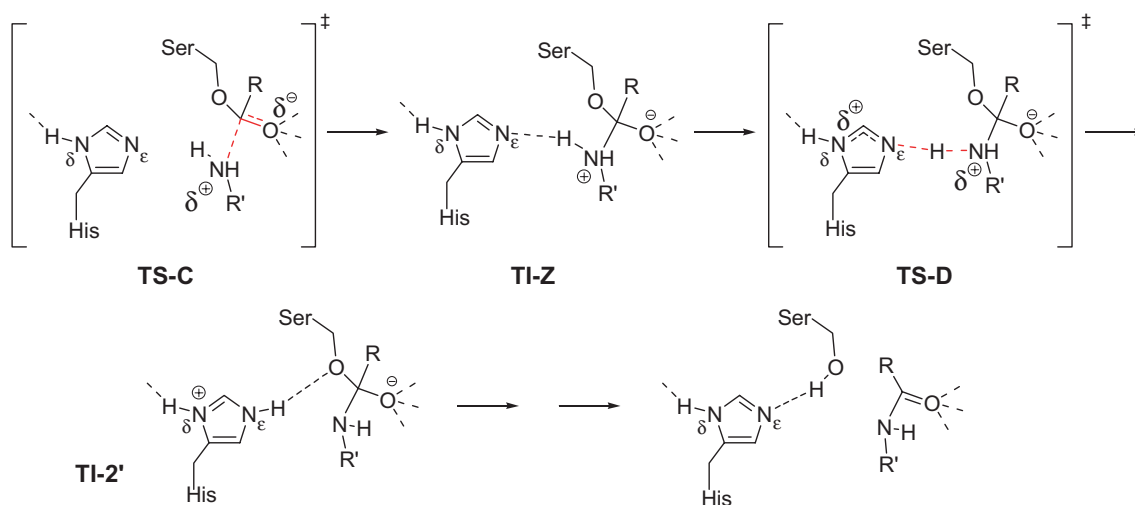
Entry	TI	Compound	H-bond distance, Å (angle, °) <sup>a</sup>					
			a	b	c or c'	d	e	f
1	TI-2	(1 <i>R</i> ,2 <i>S</i> )-1	2.97 (132)	2.84 (145)	<b>3.49 (148)</b>	2.87 (151)	2.78 (175)	2.95 (173)
2	TI-Z	(1 <i>R</i> ,2 <i>S</i> )-1	2.80 (149)	— <sup>b</sup>	3.17 (138)	2.92 (154)	2.78 (176)	3.00 (170)
3	TI-Z	(1 <i>S</i> ,2 <i>R</i> )-1	2.83 (165)	— <sup>b</sup>	<b>3.96 (90)</b>	2.87 (151)	2.80 (167)	2.78 (170)
4	TI-Z	(1 <i>R</i> ,2 <i>R</i> )-2	2.89 (166)	— <sup>b</sup>	3.12 (125)	3.08 (161)	2.83 (172)	2.82 (173)
5	TI-Z	(1 <i>S</i> ,2 <i>S</i> )-2	2.88 (164)	— <sup>b</sup>	3.18 (125)	3.13 (160)	2.74 (165)	<b>3.28 (128)</b>
6	TI-Z	(1 <i>R</i> ,2 <i>S</i> )-5	2.87 (169)	— <sup>b</sup>	2.90 (131)	3.27 (141)	2.77 (155)	2.97 (163)
7	TI-Z	(1 <i>S</i> ,2 <i>R</i> )-5	2.87 (166)	— <sup>b</sup>	2.94 (125)	3.17 (159)	2.77 (171)	2.78 (173)

<sup>a</sup> Figure 2 defines the hydrogen bonds. Distances are between heteroatoms involved in the H-bonds (N–N, N–O, O–O), and angles refer to the N–H–O or similar. Lost hydrogen bonds appear in bold.

<sup>b</sup> Not relevant for TI-Z (see Fig. 2B).



**Scheme 2.** An example of the stepwise mechanism through zwitterionic intermediates for the aminolysis reaction of **6**.<sup>22</sup> The acyl-enzyme intermediate in the serine-mediated mechanism could be visualised as an analogue to compound **6**.



**Scheme 3.** Proposed mechanism through zwitterionic intermediates for the lipase-catalysed aminolysis.

Figure 2B (a, c', d–f). Starting from the best phosphoramidate obtained for TI-2 for the fast-reacting enantiomer, we built and modelled the protonated intermediate for (1*R*,2*S*)-**1** (see details in Experimental), obtaining the structure that is shown in Figure 3A.

The methyl of the acetate lies in the large subsite, while the carbocycle was perfectly bound into the medium-sized pocket, with the phenyl ring in a pseudo-equatorial position at the fold of the envelope and the amino group at the flap in a nearly equatorial disposition. This conformation was also the most stable found using DFT calculations (Becke3LYP/6-31+G\* level of theory; see Fig. 4A).<sup>26</sup> The phenyl moiety was placed near to the right side of the large hydrophobic subsite, allowing the existence of favourable van der Waals interactions with Ile189 and Ile285. As shown in Table 2 (entry 2), the distance between the N<sub>ε</sub> of His224 and the amine diminished and was appropriate for the existence of the H-bond (bond c'). Furthermore, all five essential hydrogen bonds were present and no steric impediments between the substrate and the lipase were found.

To verify the validity of this novel intermediate, we next built and modelled the TI-Z analogue for the slow-reacting enantiomer (1*S*,2*R*)-**1**, and the obtained results were in agreement with the experimental facts. The best conforma-

tion obtained is shown in Figure 3B. In it, the cyclopentane presented a more unstable distorted envelope conformation and it was shared out between the medium and the large pockets, with the phenyl hydrophobic group pointing towards the solvent. Moreover, the distance between the N<sub>ε</sub> of His224 and the N of the protonated amine was too large (bond c', Table 2, entry 3). Thus, the best conformation of the cycle for (1*R*,2*S*)-**1** and its improved disposition into the active site of the lipase (better TS-C), as well as the loss of one of the key hydrogen bonds in the intermediate of (1*S*,2*R*)-**1** (and therefore, worse TS-D) can explain the excellent enantioselectivity obtained in the resolution of *rac*-**1**.

The CAL-B-catalysed resolution of (±)-*cis*-2-phenylcyclopentanamine *rac*-**2** was not as efficient as in the case of the *trans*-isomer, although the (1*R*,2*R*) enantiomer reacted 16 times faster than the *S* one (Table 1, entry 2).<sup>11a</sup> To explain these differences, we built and modelled the zwitterionic intermediates for both enantiomers of the *cis* isomer *rac*-**2**. Thus, in the best conformation obtained for the fast-reacting enantiomer (1*R*,2*R*)-**2** (Fig. 3C), the carbocycle was bound into the medium-sized pocket in a conformation slightly different from the most stable disposition found by DFT calculations (Fig. 4B).<sup>26</sup> The amino group was placed at the flap of the envelope in a pseudo-axial position and the phenyl ring at the fold of the envelope

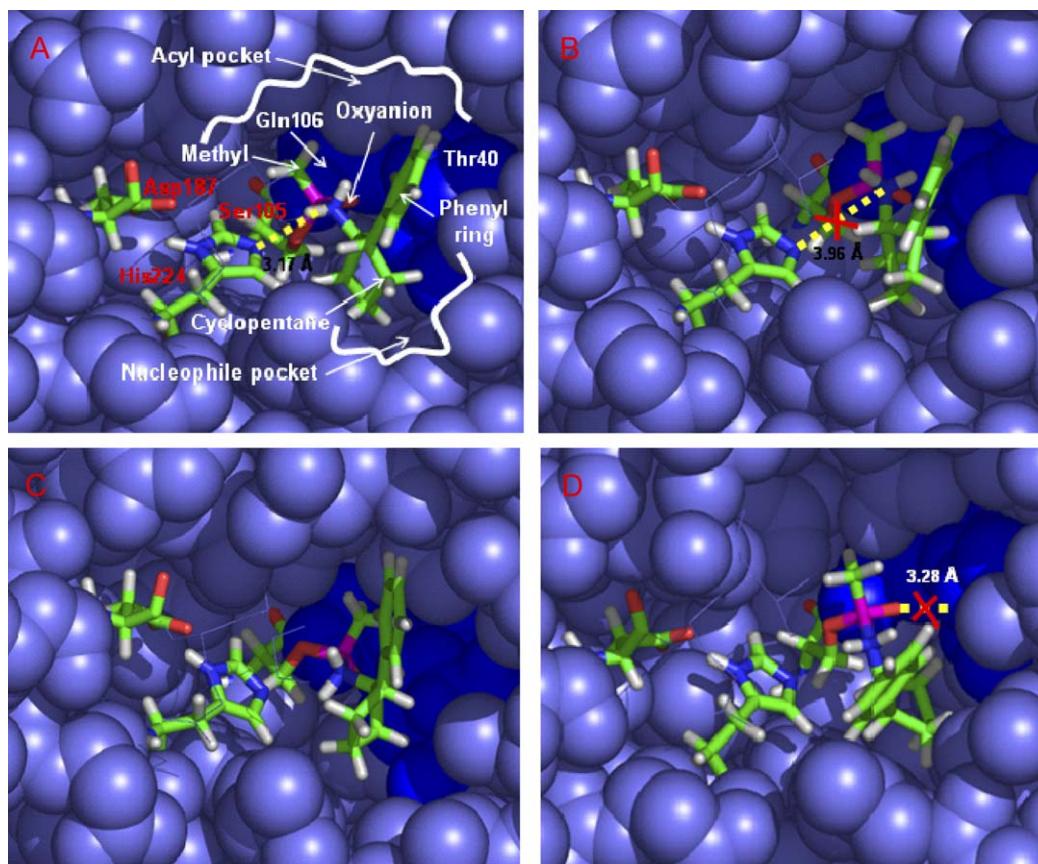


**Figure 3.** The best conformations of the analogues for: (A) TI-Z of (1*R*,2*S*)-1; (B) TI-Z of (1*S*,2*R*)-1; (C) TI-Z of (1*R*,2*R*)-2 and (D) TI-Z of (1*S*,2*S*)-2. Lost key-hydrogen bonds appear with a red cross. The above images display Glu188 and Ile189 in a line representation to allow a better view of the large pocket of the lipase.

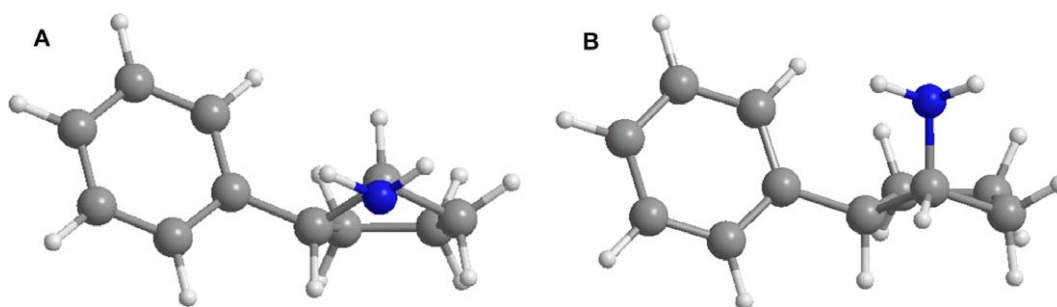


**Figure 4.** Main conformation using DFT calculations for: (A) *rac*-1 and (B) *rac*-2.

fitted in a nearly equatorial disposition pointing out to the solvent. The interaction between the catalytic histidine and the ammonium group was not very strong since the angle was scarcely higher than  $120^\circ$  (bond *c'*, Table 2, entry 4). We think that these facts could be an explanation for the 7-fold lower reactivity of this enantiomer compared to the *trans* isomer (1*R*,2*S*)-1.

Next, we searched for a productive conformation of the TI-Z analogue for the enantiomer (1*S*,2*S*)-2, but we did not find it (Fig. 3D). For the best one, the cyclopentane presented a distorted envelope conformation with both substituents in pseudo-equatorial positions. Furthermore, the

phenyl ring was closer to His224 forcing the substrate to move next to Thr40, thus losing an H-bond interaction (bond *f*, Table 2, entry 5). This loss of one of the key hydrogen bonds for the catalysis and the less adequate disposition of the substrate can explain the worse reactivity of (1*S*,2*S*)-2, and, therefore, the enantioselectivity exhibited by the enzyme.

## 2.2. *trans*-2-Phenylcyclopropanamine *rac*-5

As shown previously (Table 1, entry 5), CAL-B catalysed the acetylation of *rac*-5 with high efficiency (90% of the conversion was obtained after 2 h of reaction) but with

very low enantioselectivity ( $E = 4$ ), that is, both enantiomers were good substrates for the lipase.<sup>11b</sup> When we built and minimised the TI-Z analogues for both enantiomers of *rac-5*, the results obtained were in good agreement with those of the experimental (Table 2, entries 6 and 7). Both structures presented all key-hydrogen bonds with no intra- or inter-molecular steric clashes. The smaller size of the carbocycle allowed a minor distance between the catalytic histidine and the ammonium group (bond  $c'$ , around 2.90 Å), and thus, a very efficient H-bond interaction.

The protonated phosphoramidate of the enantiomer (1*R*,2*S*)-**5** (Fig. 5A) showed a disposition in the active site similar to that for (1*R*,2*S*)-**1** (Fig. 3A), with the phenyl group on the right side of the large hydrophobic pocket pointing out to the solvent but, interestingly, the intermediate for (1*S*,2*R*)-**5** (Fig. 5B) presented a more favoured unexpected binding of the phenyl moiety with regards to the five-membered analogue (1*S*,2*R*)-**1** (compare with Fig. 3B). The smaller size of the cycle of (1*S*,2*R*)-**5** allowed

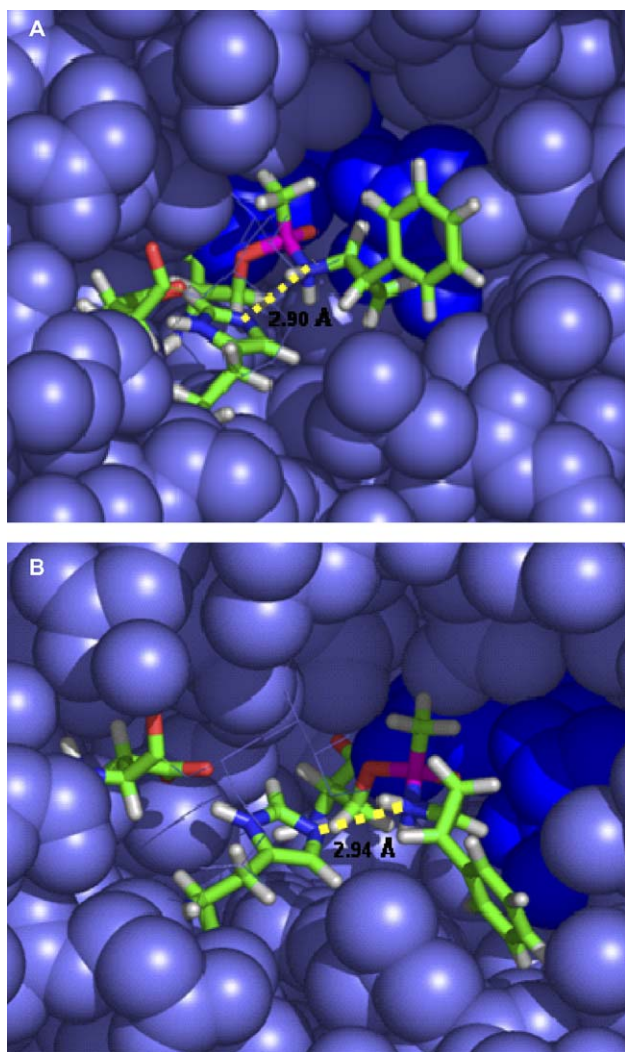


**Figure 5.** Best conformations of the analogues for: (A) TI-Z of (1*R*,2*S*)-**5** and (B) TI-Z of (1*S*,2*R*)-**5**. The above images display Glu188 and Ile189 in a line representation to allow a better view of the large pocket of the lipase.

the phenyl ring to be deeply fitted into the medium subsite, thus making favourable van der Waals interactions with the hydrophobic side chains of Trp104, Leu278, Ala282 and Ile285. These results indicate that modelling of the TI-Z analogues can also predict the poor resolution of *rac-5*, because both enantiomers can bind perfectly into the active site of CAL-B.

### 2.3. 2-Phenylcyclohexanamines *rac-3* and *rac-4*

Next, we studied the CAL-B-catalysed acylation of ( $\pm$ )-*trans*-2-phenylcyclohexanamine *rac-3*. This compound was efficiently resolved with CAL-B<sup>11b</sup> and ethyl acetate but, significantly, this process was much slower than that with ( $\pm$ )-*trans*-2-phenylcyclopentanamine *rac-1* (Table 1, entries 1 and 3).<sup>27</sup> Cyclohexane derivatives are present in a two chair-equilibrium in solution, which lies on the side of the thermodynamically more stable one. *trans*-1,2-Disubstituted derivatives virtually exist only in this conformation placing both substituents in equatorial positions. Thus, only those structures with both the amino and the phenyl groups placed at equatorial positions were taken into account during the computer modelling study of *rac-3*.<sup>28</sup>

Since good results had been obtained using the zwitterionic intermediates, we built and minimised the corresponding one for the fast-reacting enantiomer (1*R*,2*S*)-**3**. However, although we systematically searched for several dispositions of the cycle, the H-bond between the  $N_{\epsilon}$  of the catalytic histidine and the ammonium group (bond  $c'$ , see Fig. 2B) was always lost, being 3.32 Å the shortest distance found (Table 3, entry 1), indicating that the direct proton transfer between both groups would not be favoured.

To be plausible as catalytically productive intermediates, this mechanism should provide an alternative path for this proton transfer. Previous reports based on modelling studies have suggested that a proton can be carried between the catalytic His and the nucleophile/leaving group by means of another molecule, which would act as a proton transfer (PT, Fig. 6). Thus, proton transfer-aided pathways have been previously proposed for the CAL-B-catalysed enantioselective ring opening of  $\beta$ -lactams,<sup>29</sup> and for the CAL-B-catalysed regioselective aminolysis of 3',5'-diaminonucleosides.<sup>15</sup>

Although reactions were performed with anhydrous solvents, and amines were stored under a nitrogen atmosphere, in all cases the acyl donor was partially hydrolysed, such as that indicated by analysis of the <sup>1</sup>H NMR spectra of the reaction crudes.<sup>30</sup> Thus, either ethanol coming from ethyl acetate or water present in the medium reaction could play the role of a proton transfer.<sup>31</sup> Starting from the TI-Z analogue obtained for (1*R*,2*S*)-**3**, we first modelled an ethanol molecule in different positions near the catalytic triad, obtaining as the most stable structure the one in which this molecule was midway between the protonated amine and the catalytic histidine. Although the substrate fitted correctly into the active site, the calculated  $N_{\epsilon}$ -O distance was too large (bond  $g$ , 4.14 Å) for the existence of an H-bond interaction (Table 3, entry 2).

**Table 3.** Distances and angles of the key hydrogen bonds in the most productive conformations obtained for the intermediates in the CAL-B-catalysed acetylation of *rac*-3 and *rac*-4

Entry	Compound	H-bond distance, Å (angle, °) <sup>a</sup>						
		a	c'	d	e	f	g	h
1	(1 <i>R</i> ,2 <i>S</i> )-3	2.81 (155)	<b>3.32 (131)</b>	2.92 (156)	2.80 (170)	2.92 (172)	— <sup>b</sup>	— <sup>b</sup>
2	(1 <i>R</i> ,2 <i>S</i> )-3	2.82 (158)	— <sup>c</sup>	2.93 (148)	2.77 (178)	3.28 (167)	<b>4.14 (161)</b>	3.17 (152)
3	(1 <i>R</i> ,2 <i>S</i> )-3	2.82 (158)	— <sup>c</sup>	2.87 (146)	2.75 (179)	3.07 (171)	3.34 (166)	2.96 (160)
4	(1 <i>S</i> ,2 <i>R</i> )-3	2.83 (156)	— <sup>c</sup>	2.91 (146)	2.77 (167)	2.80 (173)	<b>3.29 (126)</b>	3.06 (139)
5	(1 <i>R</i> ,2 <i>R</i> )-4	2.87 (172)	— <sup>c</sup>	3.12 (163)	2.83 (168)	2.80 (172)	<b>3.51 (136)</b>	3.18 (140)
6	(1 <i>S</i> ,2 <i>S</i> )-4	2.84 (169)	— <sup>c</sup>	3.02 (160)	3.03 (160)	2.79 (164)	<b>3.41 (134)</b>	3.25 (133)

<sup>a</sup> Figures 2B and 6 define the hydrogen bonds. Distances are between heteroatoms involved in the H-bonds (N–N, N–O, O–O), and angles refer to the N–H–O or similar. Lost hydrogen bonds appear in bold.

<sup>b</sup> This H-bond is not present in TI-Z (see Fig. 2B).

<sup>c</sup> This distance is not present in 'assisted TI-Z' (see Fig. 6).

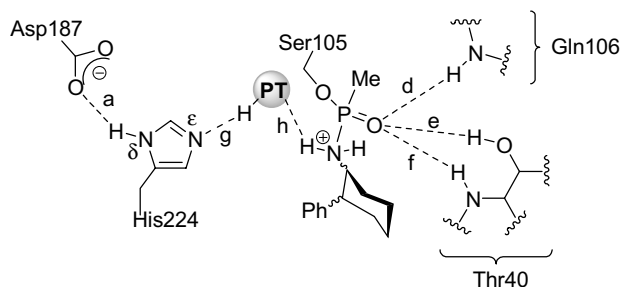


**Figure 6.** Analogues of 'assisted TI-Z' used in the molecular modelling study for the acetylation of 2-phenylcyclohexanamines catalysed by CAL-B. Essential hydrogen bonds for the catalysis are shown as dashed lines (a–h). Novel interactions are now named as g and h. PT = proton transfer.

Better results were obtained when a molecule of water was added as PT and modelled in several positions close to the catalytic triad. We found a stable intermediate with a similar binding of the substrate in the active site of the lipase (Fig. 7A) to that obtained in the ethanol-assisted TI-Z, where the smaller size of the water molecule allowed that all key-hydrogen bonds were present in the intermediate (Table 3, entry 3).<sup>32</sup>

Next, we modelled the analogue of 'assisted TI-Z' with a molecule of water for the slow-reacting enantiomer (1*S*,2*R*)-3, but no adequate conformations were found (Fig. 7B). In all cases, the interaction between His224 and the molecule of water was very weak or was not present (bond g, Table 3, entry 4). Furthermore, the comparison of the modelled intermediates for both enantiomers (Fig. 8) shows for (1*S*,2*R*)-3 a worse binding of the phenyl moiety in the acyl subsite. Thus, in analogy, the phenyl group was placed close to both the catalytic histidine and the molecule of water (average phenyl–water distance: 5.25 Å), meanwhile in the (1*R*,2*S*)-3 intermediate, this group was fitted on the right side of the large pocket, moving from the proton transfer (average phenyl–water distance: 5.70 Å) and leaving free the space over His224. So, in this case, modelling predicts that a PT is necessary to transfer the proton from the nucleophile to the catalytic histidine. Better bindings of the substrate and the molecule of water in the (1*R*,2*S*)-3 intermediate can justify the enantiopreference exhibited by CAL-B towards this substrate.

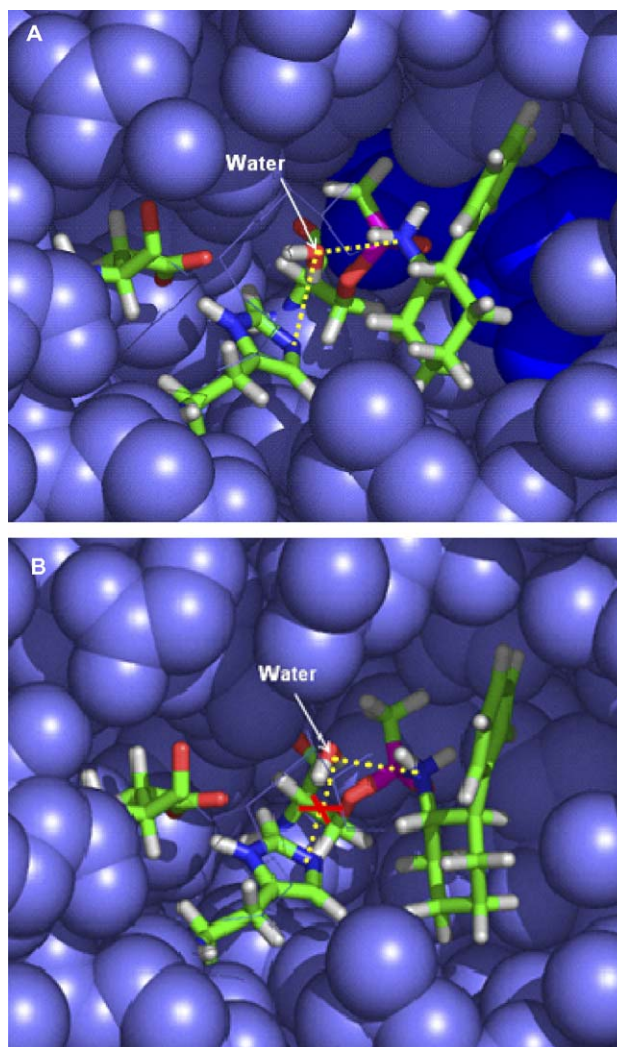


**Figure 7.** Best conformations of the analogues for: (A) 'assisted TI-Z' with a molecule of water of (1*R*,2*S*)-3 and (B) 'assisted TI-Z' with a molecule of water of (1*S*,2*R*)-3. Lost key-hydrogen bond appears with a red cross. The above images display Glu188 and Ile189 in a line representation to allow a better view of the large pocket of the lipase.

Finally, we studied the enzymatic resolution of *rac*-4. This amine proved to be a very poor substrate for CAL-B, since after 2 days of reaction, only 5% of amine was converted

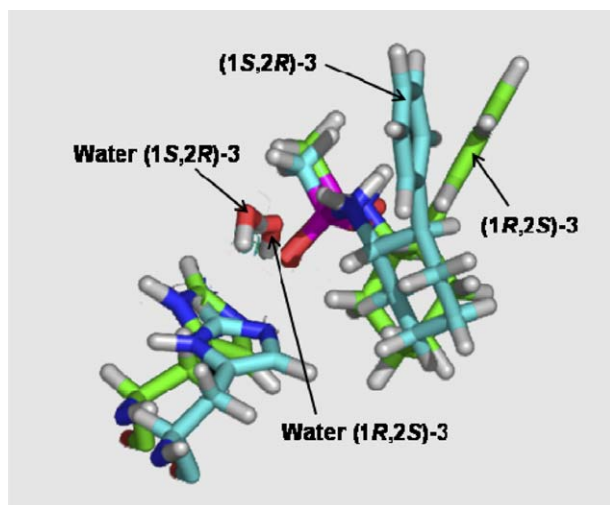


**Figure 8.** Structural comparison of ‘assisted TI-Z’ analogues of (1*R*,2*S*)-3 (green) and (1*S*,2*R*)-3 (blue) with a molecule of water acting as a proton transfer. The phenyl moiety in the (1*S*,2*R*)-3 structure was closer to the molecule of water, hindering a good fitting of the proton transfer.

into the acetamide of very low *ee* (13%, Table 1, entry 4).<sup>11b</sup> To carry out the modelling of the corresponding intermediate derived from *rac*-4, we have only taken into account the conformation observed in the <sup>1</sup>H NMR spectrum of amine *rac*-4. Analysis of the coupling constants values measured for the signals of H-1 and H-2 indicated an equatorial position for the phenyl group and an axial position for the amino group.<sup>33</sup>

By analogy with the *trans* isomer *rac*-3, the water proton transfer-assisted model was used for the *cis*-isomer *rac*-4. We searched for productive conformations of (1*R*,2*R*)-4 analogue, but in the best structure found, the carbocycle rotated pointing the axial hydrogens H-3 and H-5 towards the catalytic histidine and placing the phenyl group in the acyl pocket exposed to the solvent. Due to the *cis* arrangement of phenyl and amino groups, the aromatic ring was placed very close to the molecule of water (average phenyl–water distance: 4.95 Å). As a result, the binding of the water molecule was destabilised, thus losing an H-bond interaction (bond g, Table 3, entry 5).

When the ‘assisted TI-Z’ model with a molecule of water for (1*S*,2*S*)-4 was built and minimised, the best structure obtained showed that the cyclohexane was not bound into the medium pocket and the phenyl moiety was in the acyl subsite extending some parts into the solvent. In this case, although the phenyl ring was not as close to the molecule of water (average phenyl–water distance: 5.60 Å), the H-bond interaction with His224 was lost (bond g, Table 3, entry 6).

For *rac*-4, the proton transfer-aided model can also explain its poor reactivity. For both enantiomers, the substrate did not fit well into the lipase active-site and the transport of the proton from the nucleophile to the catalytic histidine seems to be hindered.

### 3. Conclusions

Results obtained in the enzymatic resolution of some 2-phenylcycloalkanamines catalysed by CAL-B show that the size of the cycle and the relative configuration of the chiral centres play an important role in determining both the reaction rate and the enantioselectivity. Molecular modelling studies on the aminolysis of these 2-phenylcycloalkanamines 1–5 suggest the favoured formation of zwitterionic intermediates resulting from the direct attack of the amine to the carbonyl group of the acyl-enzyme without the activation of the catalytic histidine, which is in contrast to the concerted pathway predicted in the serine-mediated mechanism. In a second step, deprotonation of the formed ammonium group by the catalytic histidine would take place. Alternatively, a molecule of water to assist the transfer of the proton could be necessary.

Furthermore, this computer-aided modelling study can also explain the different reaction rates observed in these enzymatic processes. Thus, the requirement of a molecule of water to transport a proton from the nucleophile to the catalytic histidine could be responsible for the lower reaction rate of the *trans*-cyclohexanamine *rac*-3 with regards to its cyclopentyl and cyclopropyl analogues. Finally, the poor reactivity of *rac*-4 has also been explained, because in its major ring conformation, the binding of both enantiomers does not allow an adequate transfer of the proton to the histidine.

### 4. Experimental

The program Insight II, version 2000.1, was used for viewing the structures. The geometric optimisations were performed using Discover, version 2.9.7 (*Accelrys*, San Diego CA, USA), using the AMBER force field.<sup>18</sup> The distance dependent dielectric constant was set to 4.0 to mimic the electrostatic shielding of the solvent and the 1–4 van der Waals interactions were scaled to 50%. The crystal structure for the CAL-B (1lbs)<sup>17</sup> was obtained from the Protein Data Bank ([www.rcsb.org/pdb/](http://www.rcsb.org/pdb/)), and includes a phosphonate. Protein structures shown in this paper were created using PyMol v0.97.

The crystal structure of CAL-B was relaxed before the addition of the substrate to the experimental structure. The PDB file 1lbs was opened with all the atoms of the crystal structure, including water molecules. Hydrogen atoms were added to the structure using a Biopolymer module, tested for partial charge balance and corrected for atom types within the AMBER force field. Geometry optimisations were carried out in two steps. First, the steepest descent algorithm corrected major high energy structural problems and got the molecule to a local minimum with a RMS deviation of about 0.02 Å mol<sup>-1</sup>. Second, conjugate gradient algorithm gave a faster and more precise minimisation near the local minima, obtaining a RMS value of 0.005 Å mol<sup>-1</sup> or lower. The entire structure was relaxed by a systematic manner that avoided large structural changes. First only the water molecules were



optimised. Afterwards, the side chains of the amino acids were released and optimised as well. The entire complex of the enzyme and solvent molecules was then released for the final optimisation. For all further geometry optimisations in this study, the solvent molecules were never fixed. This was to ensure that water molecules were mobile and that their position did not hinder the substrate.

#### 4.1. Geometry optimisation of phosphoramidate core

A phosphoramidate core of the tetrahedral intermediate mimicking acetylation of ethylamine was assembled manually in the crystal structure. The partial charges on the intermediate atoms were set to those of the tetrahedral intermediate (carbon, not phosphorus), the values of which were obtained by semi-empirical calculation performed using the AM1 parameters.

At this stage, the proton linked to the nucleophile amine was minimised in the two possible positions where it can be placed since it can interconvert its position with the electron lone-pair in order to choose the best intermediate.

For the optimisation of the phosphoramidate core, a systematic approach of releasing different motifs was applied. Initially, the intermediate was allowed to adjust to the enzyme active site by keeping the entire enzyme fixed during the geometry optimisation. The side chains of the lipase were then released and allowed to adjust and finally the entire complex was allowed to adjust. This approach avoided drastic changes in the lipase structure caused by non-optimal conformations of the intermediate. A hydrogen bond calculation was performed after each minimisation in order to assure the presence of the critical hydrogen bonds around the catalytic site.

#### 4.2. Phosphoramidate analogues of TI-2 including 2-phenyl-cycloalkanamine group

After obtaining a catalytically productive intermediate core, the remainder of the cyclic amine was added, firstly the cycle and then the phenyl group, and different conformations were produced by manual adjustment of dihedral angles identified in Figure 9. Geometry optimisations were again performed using the same approach used to optimise the phosphoramidate core with systematic releasing of the substrate, amino acid side chains and the entire enzyme complex. Again, minimisations were carried out with both the steepest descent and conjugate gradients until an RMS value of at least  $0.005 \text{ \AA mol}^{-1}$  was obtained.

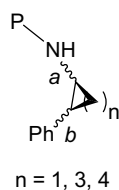


**Figure 9.** Manipulated dihedral angles for 2-phenylcycloalkanamine structures. Dihedral angles corresponding to all the bonds labelled above were adjusted during manual conformational searching.

Adjustments of approximately  $10\text{--}20^\circ$  were performed for dihedral angles involving a and b bonds when a local minima structure was found. Structures with obvious steric problems were ignored. Additional manual adjustments were done to orient substrate moieties into visible pockets.

#### 4.3. Zwitterionic intermediates (TI-Z)

To obtain these structures, the amino group was replaced by an ammonium fragment, and the catalytic histidine deprotonated, that is, we started minimising the acetylation of ethylammonium, and then we built the rest of the molecule, first, the cycle and then the phenyl moiety. For the optimisation of the zwitterionic core, the same systematic approach of releasing was applied. First, only the intermediate was allowed to adjust to the enzyme active site. Second, the side chains of the amino acids were released too, and finally the entire complex was allowed to adjust, allowing the molecules of water to adjust their position in all steps.

Adjustments of approximately  $10\text{--}20^\circ$  were performed for dihedral angles when a local minima structure was found. Structures with obvious steric problems were ignored. Additional manual adjustments were carried out in order to orient substrate moieties into visible pockets.

#### 4.4. ‘Assisted’ zwitterionic intermediates

Finally, in the TI-Z analogues obtained for 2-phenylcyclohexanamines, a molecule of ethanol or water was added in several positions near from the catalytic histidine. For the optimisation of this structure, a similar systematic approach of releasing was applied. First, only the proton transfer was allowed to adjust to the enzyme structure. Second, the substrate and the side chains of the amino acids were released too, and finally the entire complex was allowed to adjust, with all the molecules of water releasing in each step.

#### Acknowledgements

This work has been supported by MEC (Spain; Project MEC-04-CTQ-04185). J.G.-S. thanks the Spanish MEC for a predoctoral fellowship. The authors also thank Romas Kazlauskas (University of Minnesota) and Wolfgang Kroutil (University of Graz) for critical reading of the manuscript.

#### References

- Um, I.-K.; Hong, J.-Y.; Seok, J.-A. *J. Org. Chem.* **2005**, *70*, 1438–1444, and references cited therein.
- Bruice, T. C.; Mayahi, M. F. *J. Am. Chem. Soc.* **1960**, *82*, 3067–3071.
- Jencks, W. P.; Carriuolo, J. *J. Am. Chem. Soc.* **1960**, *82*, 675–681.
- Bunnett, J. F.; Davis, G. T. *J. Am. Chem. Soc.* **1960**, *82*, 665–674.
- (a) Alfonso, I.; Gotor, V. *Chem. Soc. Rev.* **2004**, *33*, 201–209; (b) van Rantwijk, F.; Sheldon, R. A. *Tetrahedron* **2004**, *60*,

- 501–519; (c) Breuer, M.; Dittrich, K.; Habicher, T.; Hauer, B.; Keßeler, M.; Stümer, R.; Zelinski, T. *Angew. Chem., Int. Ed.* **2004**, *43*, 788–824; (d) Gotor, V. *Bioorg. Med. Chem.* **1999**, *7*, 2189–2197.
6. (a) Skupinska, K. A.; McEachern, E. J.; Baird, I. R.; Skerlj, R. T.; Bridger, G. J. *J. Org. Chem.* **2003**, *68*, 3546–3551; (b) Choi, Y. K.; Kim, M. J.; Ahn, Y.; Kim, M.-J. *Org. Lett.* **2001**, *3*, 4099–4101; (c) López-Serrano, P.; Jongejan, J. A.; Rantwijk, F.; Sheldon, R. A. *Tetrahedron: Asymmetry* **2001**, *12*, 219–228; (d) Takayama, S.; Lee, S. T.; Hung, S.-C.; Wong, C.-H. *Chem. Commun.* **1999**, 127–128; (e) Messina, F.; Botta, M.; Corelli, F.; Schneider, M. P. *J. Org. Chem.* **1999**, *64*, 3767–3769; (f) Soledad de Castro, M. S.; Sinisterra Gago, J. V. *Tetrahedron* **1998**, *54*, 2877–2892; (g) Öhrner, N.; Orrenius, C.; Mattson, A.; Norin, T.; Hult, K. *Enzyme Microb. Technol.* **1996**, *19*, 328–331; (h) Reetz, M. T.; Schimossek, K. *Chimia* **1996**, *50*, 668–669; (i) Puertas, S.; Brieva, R.; Rebolledo, F.; Gotor, V. *Tetrahedron* **1993**, *49*, 4007–4014.
7. (a) Balkenhohl, F.; Dittrich, K.; Hauer, B.; Ladner, W. *J. Prakt. Chem.* **1997**, *339*, 381–384; (b) Balkenhohl, F.; Hauer, B.; Ladner, W.; Pressler, U. (BASF AG), DE 4332738, 1993; *Chem. Abstr.* **1995**, *122*, 289035; (c) Dittrich, K.; Balkenhohl, F.; Ladner, W. (BASF AG), DE 19534208, **1995**; *Chem. Abstr.* **1997**, *126*, 277259.
8. (a) Hedstrom, L. *Chem. Rev.* **2002**, *102*, 4501–4523; (b) Fersht, A. R. *Enzyme Structure and Mechanism*, 2nd ed.; Freeman: Nueva York, 1985.
9. (a) González-Sabín, J.; Gotor, V.; Rebolledo, F. *Chem. Eur. J.* **2004**, *10*, 5788–5794; (b) González-Sabín, J.; Gotor, V.; Rebolledo, F. *Tetrahedron: Asymmetry* **2002**, *13*, 1315–1320; (c) Sánchez, V. M.; Rebolledo, F.; Gotor, V. *J. Org. Chem.* **1999**, *64*, 1464–1470; (d) Alfonso, I.; Astorga, C.; Rebolledo, F.; Gotor, V. *Chem. Commun.* **1996**, 2471–2472.
10. Lavandera, I.; Fernández, S.; Ferrero, M.; Gotor, V. *J. Org. Chem.* **2001**, *66*, 4079–4082.
11. (a) González-Sabín, J.; Gotor, V.; Rebolledo, F. *Tetrahedron: Asymmetry* **2004**, *15*, 481–488; (b) González-Sabín, J.; Gotor, V.; Rebolledo, F. *Tetrahedron: Asymmetry* **2005**, *16*, 3070–3076.
12. Thus, *trans*-2-phenylcyclopentanamine **1**, ‘cypenamine’ and *trans*-2-phenylcyclopropanamine **5**, ‘tranylcypromine’ are well-known antidepressants: McGrath, W. R.; Kuhn, W. L. *Arch. Int. Pharmacodyn. Ther.* **1968**, *172*, 405–413; Riley, T. N.; Brier, C. G. *J. Med. Chem.* **1972**, *15*, 1187–1188. In addition, *cis* and *trans*-isomers of 2-phenylcyclopentanamine and 2-phenylcyclohexanamine **1–4** are building blocks of semi-cyclic amidines with potent hypoglycaemic activity: Hartmann, S.; Ullrich, S.; Hupfer, C.; Frahm, A. W. *Eur. J. Med. Chem.* **2000**, *35*, 377–392; Grisar, J. M.; Claxton, G. P.; Carr, A. A.; Wiech, N. L. *J. Med. Chem.* **1973**, *16*, 679–683. They have also been used as starting materials in the synthesis of sulfonamides potentiators of AMPA receptors, the activity being dependent on the stereochemistry of the stereogenic centres: 12 Shepherd, T. A.; Aikins, J. A.; Bleakman, D.; Cantrell, B. E.; Rearick, J. P.; Simon, R. L.; Smith, E. C. R.; Stephenson, G. A.; Zimmerman, D. M. *J. Med. Chem.* **2002**, *45*, 2101–2111.
13. Kazlauskas, R. J.; Weissfloch, A. N. E.; Rappaport, A. T.; Cuccia, L. A. *J. Org. Chem.* **1991**, *56*, 2656–2665.
14. Similar rates of reaction were observed in the lipase-catalysed transesterification of some *cis*-2-substituted cyclohexanols but, in contrast with the aminolysis reaction, processes catalysed by CAL-B showed very high enantioselectivities in some cases. For instance, see: (a) Levy, L. M.; Lavandera, I.; Gotor, V. *Org. Biomol. Chem.* **2004**, *2*, 2572–2577; (b) Levy, L. M.; Dehli, J. R.; Gotor, V. *Tetrahedron: Asymmetry* **2003**, *14*, 2053–2058; (c) Tanikaga, R.; Matsumoto, Y.; Sakaguchi, M.; Koyama, Y.; Ono, K. *Tetrahedron Lett.* **2003**, *44*, 6781–6783; (d) Brunet, C.; Zarevucka, M.; Wimmer, Z.; Legoy, M.-D. *Enzyme Microb. Technol.* **2002**, *31*, 609–614; (e) Forró, E.; Kanerva, L. T.; Fülöp, F. *Tetrahedron: Asymmetry* **1998**, *9*, 513–520; (f) Luna, A.; Astorga, C.; Fülöp, F.; Gotor, V. *Tetrahedron: Asymmetry* **1998**, *9*, 4483–4487.
15. Lavandera, I.; Fernández, S.; Magdalena, J.; Ferrero, M.; Kazlauskas, R. J.; Gotor, V. *ChemBioChem* **2005**, *6*, 1381–1390.
16. (a) Hult, K.; Berglund, P. *Curr. Opin. Biotechnol.* **2003**, *14*, 395–400; (b) Kazlauskas, R. *Science* **2001**, *293*, 2277–2278; (c) Kazlauskas, R. J. *Curr. Opin. Chem. Biol.* **2000**, *4*, 81–88; (d) Hæffner, F.; Norin, T. *Chem. Pharm. Bull.* **1999**, *47*, 591–600.
17. Uppenberg, J.; Öhrner, N.; Norin, M.; Hult, K.; Kleywegt, G. J.; Patkar, S.; Waagen, V.; Anthonsen, T.; Jones, T. A. *Biochemistry* **1995**, *34*, 16838–16851.
18. (a) Cornell, W. D.; Cieplak, P.; Bayly, C. I.; Kollmann, P. A. *J. Am. Chem. Soc.* **1993**, *115*, 9620–9631; (b) Weiner, S. J.; Kollman, P. A.; Case, D. A.; Singh, U. C.; Ghio, C.; Alagona, G.; Profeta, S.; Weiner, P. *J. Am. Chem. Soc.* **1984**, *106*, 765–784.
19. (a) Uppenberg, J.; Patkar, S.; Bergfors, T.; Jones, T. A. *J. Mol. Biol.* **1994**, *235*, 790–792; (b) Uppenberg, J.; Hansen, M. T.; Patkar, S.; Jones, T. A. *Structure* **1994**, *2*, 293–308.
20. (a) Luić, M.; Tomić, B.; Lešćić, I.; Šepac, D.; Šunjić, V.; Vitale, L.; Saenger, W.; Kojić-Prodić, B. *Eur. J. Biochem.* **2001**, *268*, 3964–3973; (b) Cygler, M.; Grochulski, P.; Kazlauskas, R. J.; Schrag, J. D.; Bouthillier, F.; Rubin, B.; Serreqi, A. N.; Gupta, A. K. *J. Am. Chem. Soc.* **1994**, *116*, 3180–3186.
21. To identify the hydrogen bonds, a donor atom to acceptor atom distance of less than 3.20 Å and a donor atom–hydrogen–acceptor atom angle >120° are required.
22. Adalsteinsson, H.; Bruice, T. C. *J. Am. Chem. Soc.* **1998**, *120*, 3440–3447.
23. In a very recent paper, we have already shown that similar zwitterionic species could act as intermediates for lipase-catalysed aminolysis reaction (see Ref. 15).
24. To differentiate between TI-2 and this new TI, we call this TI as zwitterionic since both charges are located in atoms linked to the same carbon atom.
25. Note that this intermediate is the same as TI-2 shown in Scheme 1 with the only exception being the lack of the H-bond interaction between the N<sub>ε</sub>-H of His224 and the N of the amine.
26. The programme Gaussian 98 was used: Frisch, M. J.; Trucks, G. W.; Schlegel, H. B.; Scuseria, G. E.; Robb, M. A.; Cheeseman, J. R.; Zakrzewski, V. G.; Montgomery, J. A., Jr.; Stratmann, R. E.; Burant, J. C.; Dapprich, S.; Millam, J. M.; Daniels, A. D.; Kudin, K. N.; Strain, M. C.; Farkas, O.; Tomasi, J.; Barone, V.; Cossi, M.; Cammi, R.; Mennucci, B.; Pomelli, C.; Adamo, C.; Clifford, S.; Ochterski, J.; Petersson, G. A.; Ayala, P. Y.; Cui, Q.; Morokuma, K.; Malick, D. K.; Rabuck, A. D.; Raghavachari, K.; Foresman, J. B.; Cioslowski, J.; Ortiz, J. V.; Stefanov, B. B.; Liu, G.; Liashenko, A.; Piskorz, P.; Komaromi, I.; Gomperts, R.; Martin, R. L.; Fox, D. J.; Keith, T.; Al-Laham, M. A.; Peng, C. Y.; Nanayakkara, A.; Gonzalez, C.; Challacombe, M.; Gill, P. M. W.; Johnson, B.; Chen, W.; Wong, M. W.; Andres, J. L.; Gonzalez, C.; Head-Gordon, M.; Replogle, E. S.; Pople, J. A. *Gaussian 98, Revision A.11.3*; Gaussian: Pittsburg, PA, 2002.
27. A similar trend has been observed with other cyclic compounds: (a) Levy, L. M.; Gotor, V. *J. Org. Chem.* **2004**, *69*, 2601–2602; (b) Forró, E.; Fülöp, F. *Tetrahedron: Asymmetry* **1999**, *10*, 1985–1993; (c) Forró, E.; Szakonyi, Z.; Fülöp, F. *Tetrahedron: Asymmetry* **1999**, *10*, 4619–4626; (d) Forró, E.; Lundell, K.; Fülöp, F.; Kanerva, L. T. *Tetrahedron: Asym-*

- metry **1997**, 8, 3095–3099; (e) Maestro, A.; Astorga, C.; Gotor, V. *Tetrahedron: Asymmetry* **1997**, 8, 3153–3159.
28. The  $^1\text{H}$  NMR spectrum of *rac*-**3** ( $\text{CDCl}_3$ ) showed two well defined signals for H-1 and H-2. Both signals (with the same splitting: ddd) showed two large  $^3J_{\text{H,H}}$  values (10–12 Hz), which are indicative of *trans*-diaxial arrangements between H-1 and H-2; H-1 and H-6ax; and H-2 and H-3ax.
  29. Park, S.; Forró, E.; Grewal, H.; Fülöp, F.; Kazlauskas, R. J. *Adv. Synth. Catal.* **2003**, 345, 986–995.
  30. Remaining substrates were obtained as mixtures of the free bases and their acetate salts.
  31. To abbreviate, we will call these structures as ‘assisted TI-Z’.
  32. Note that although bond g has a distance larger than 3.20 Å, the excellent angle interaction makes possible a weak H-bond.
  33. Some of the signals observed in the  $^1\text{H}$  NMR spectrum ( $\text{CDCl}_3$ ) of *rac*-**4**: H-1 [q,  $J = 3.0$  Hz ( $^3J_{\text{H-1,H-2}} = ^3J_{\text{H-1,H-6eq}} = ^3J_{\text{H-1,H-6ax}}$ )]; H-2 [dt,  $J = 12.5$  Hz ( $^3J_{\text{H-2,H-3ax}}$ ) and  $J = 3.1$  Hz ( $^3J_{\text{H-1,H-2}} = ^3J_{\text{H-2,H-3eq}}$ )]. The small value of  $^3J_{\text{H-1,H-6ax}}$  indicates an equatorial position for H-1, and the great value of  $^3J_{\text{H-2,H-3ax}}$  is indicative of an axial position for H-2.